

## Accepted Manuscript

Microcalorimetry of the intestinal mucus: Hydrogen bonding and self-assembly of mucin

S. Lousinian, A.R. Mackie, N.M. Rigby, C. Panayiotou, C. Ritzoulis



PII: S0141-8130(17)33922-3  
DOI: <https://doi.org/10.1016/j.ijbiomac.2018.01.185>  
Reference: BIOMAC 9017

To appear in:

Received date: 10 October 2017  
Revised date: 22 January 2018  
Accepted date: 28 January 2018

Please cite this article as: S. Lousinian, A.R. Mackie, N.M. Rigby, C. Panayiotou, C. Ritzoulis, Microcalorimetry of the intestinal mucus: Hydrogen bonding and self-assembly of mucin. The address for the corresponding author was captured as affiliation for all authors. Please check if appropriate. Biomac(2017), <https://doi.org/10.1016/j.ijbiomac.2018.01.185>

This is a PDF file of an unedited manuscript that has been accepted for publication. As a service to our customers we are providing this early version of the manuscript. The manuscript will undergo copyediting, typesetting, and review of the resulting proof before it is published in its final form. Please note that during the production process errors may be discovered which could affect the content, and all legal disclaimers that apply to the journal pertain.

**Microcalorimetry of the intestinal mucus: Hydrogen bonding and self-assembly of mucin.**

S. Lousinian<sup>3</sup>, A.R. Mackie<sup>4</sup>, N.M. Rigby<sup>4</sup>, C. Panayiotou<sup>3</sup>, C. Ritzoulis<sup>1,2\*</sup>

1. School of Food Science and Bioengineering, Zhejiang Gongshang University, Xiasha, Hangzhou, Zhejiang 310016, China.

2. Department of Food Technology, ATEI of Thessaloniki, 57400 Thessaloniki, Greece.

3. Department of Chemical Engineering, Aristotle University of Thessaloniki, 54124 Thessaloniki, Greece.

4. School of Food Science and Nutrition, University of Leeds, Leeds LS29JT, United Kingdom

\* *Corresponding author: tel: +30 2310013379; e-mail: critzou@food.teithe.gr*

*Keywords: Mucus; mucin; microcalorimetry; self-assembly; hydrogen bond*

**Abstract**

The effect of mucin hydrogen bonding on the structure of intestinal mucus has been studied with micro-differential scanning microcalorimetry ( $\mu$ -DSC), supported by spectroscopy. The experiments were performed in water–dimethyl sulfoxide (DMSO) solutions, using either water–DMSO mixtures of an appropriate DMSO content or water as blanks, as to isolate the effects of the solvent to hydrogen bonding. When using matched water–DMSO blanks, thermal events at low temperatures are linked to the negation of mucin–DMSO interactions, while events at higher temperatures are linked to the break-up of hydrogen bonds connecting the sugars of the individual macromolecules. When using a matched solvent as blank, alterations in  $C_p$ , such as increases at 10% and 15% DMSO, have been linked to the break-up and creation of quaternary structures. In the case of water as blank, a monotonic but not linear decrease in enthalpy, hence extent of hydrogen bonding, is observed. The

above are complemented by UV spectroscopy: A blue shift of the conjugated aminoacids in the presence of DMSO suggests that the inherent stability of mucin is not only due to steric volume exclusions, but also due to extensive hydrogen bonding on behalf of the sugar moieties.

## **1. Introduction**

The mucus is a highly complex medium that provides a defensive barrier across many epithelial surfaces including gastrointestinal tract. Therein it serves many functions, such as a lubricant for the food particles; a barrier to pathogens, destructive enzymes and toxic substances, and as a selectively permeable gel layer for the exchange of nutrients with the epithelium [1]. Mucins are highly glycosylated proteins, where the carbohydrate content constitutes about 80% or more of the molecule. The protein core comprises of proline, serine and threonine, organised in so-called PTS sequences. The mucin domains have extended into long rods according to the extent of the PTS sequences [2,3]. When placed on an interface, mucins are expected to orient their hydrophilic, glycosylated parts towards the aqueous (polar) phase [4]. Gastrointestinal mucus comprises two different groups of mucins, secreted and membrane-associated. MUC 2, a main component of the secreted mucins has a protein backbone comprising of two PTS sequences and other features such as von Willebrand and cystine-rich domains [5]. It has about 5200 aminoacids, and composed the only type of surface mucus of the small intestine. The protein backbone is densely covered by glycans, which serves as both a protection layer for the protein part, and a water bonding layer, resulting in the well-known gelling properties of such mucins; the gel itself comprises of flat ring-like structures that stack under each other [3].

In physico-chemical terms, digestion of a food, toxin or drug can be visualized as the direct result of the interactions between them and the mucosal barrier of the intestine. Under this rationale, a quantitative physicochemical description of the mucosal layer components, primarily the MUC 2 fraction, can allow for a thorough description of the foods, pharmaceuticals, or toxins bioabsorption,

contributing to a wide number of fields such as food digestion drug design, and hazard assessment due to the exposure in toxins.

The dominant interactions holding together the supermolecular structures of mucin are well-expected to be the hydrogen bonds, due to the very high amount of hydroxyl-rich sugars at the mucins surface. Their absolute contribution to the intra-molecular structures of mucin has recently been quantified, and found to be indeed a major contributor to mucin self-assembly [6].

The pending questions regard the exact roles of hydrogen bonding to the supermolecular mucin structures. This work aims in studying the energetics of mucin molecules by means of micro-differential scanning calorimetry ( $\mu$ -DSC), with a special emphasis on hydrogen bonding, as to provide an answer to the above question.

## **2. Materials and methods**

### **2.1 Materials**

All reagents were of analytical grade (Sigma-Aldrich, Darmstadt, Germany). Experiments were carried out using ultrapure water obtained from an ELGA PurelabFlex apparatus (ELGA Process Water, Marlow, UK)

### **2.2 Mucus isolation and purification**

Porcine jejunum epithelial surface MUC 2-rich fraction was isolated as per Round et al. (2012) [1]. The process is as follows:., fresh porcine small intestine was rinsed using phosphate buffer (67 mM, pH 6.7) containing 0.02% w/v sodium azide and a protease inhibitor cocktail (Roche Diagnostics GmbH, Mannheim, Germany) as to remove debris. Mucus was removed by mechanically scraping the epithelial surface of the intestine; more debris was removed by extracting the *ex vivo* mucus overnight at temperatures between 18–22 °C, with 10 mM sodium phosphate (pH 6.5 and containing 4M guanadinium hydrochloride, 5 mM EDTA, 5mM N-ethylmaleimide and 0.02% w/v sodium

azide). The mucus solution was then adjusted to a density of  $1.4 \text{ g mL}^{-1}$  using CsCl and was subsequently centrifuged at 55,000 rpm at  $10 \text{ }^{\circ}\text{C}$  for an overall duration of 62 h. 1 mL aliquots were sampled from this solution and its absorption at 280 nm was measured; 2  $\mu\text{L}$  of each fraction was spotted and stained with Alcian blue. UV and Alcian blue-positive aliquots were then pooled together and diluted in extraction buffer lacking guanidinium hydrochloride (as to have a final guanidinium concentration 0.5 M), the density adjusted to  $1.4 \text{ g/mL}$  using CsCl, and again centrifuged at 50 krpm at  $10 \text{ }^{\circ}\text{C}$  for 96 h. Aliquots of 1 mL were sampled and measured at 280 nm, stained with Alcian blue. The fraction at  $1.4\text{--}1.55 \text{ g mL}^{-1}$  was strongly Alcian blue-positive and displayed a very weak absorption at 280 nm, identifying it as the mucin fraction. This fraction was then freeze dried, sealed and stored for further use.

### **2.3 Micro-differential scanning calorimetry ( $\mu$ -DSC) measurements**

Micro-DSC measurements were performed using a VP-DSC (MicroCal Inc., Northampton, MA) microcalorimeter, at a temperature range of  $10^{\circ}\text{C}$  to  $120^{\circ}\text{C}$ , and at a scan rate of  $90^{\circ}\text{C h}^{-1}$ . This study involved the dissolution of purified mucus in ultra pure water (pH 7) and in dimethyl sulfoxide (DMSO)–ultra pure water mixtures of 0–20% v/v DMSO in water. DMSO was used as to induce breaking of the hydrogen bonds in the system. The reference material was either ultrapure water, or a DMSO – water mixture of the same composition as the mucin solvent for each experiment. The text clarifies the reference used for each case.

Dilution experiments were performed in a subsequent stage, aimed in probing the re-assembly of the hydrogen bonding network with the alterations of DMSO/water ratio within the same solution. Initially a mucus solution of a given DMSO/water was prepared and measured by  $\mu$ -DSC; this solution was subsequently diluted with DMSO, until its percentage was brought up to a desired level, the mucus concentrations were re-calculated, and the experiments were resumed.

## 2.4 Spectroscopy measurements

Measurements were taken over a wavelength range of 250 nm–1100 nm (UV-vis-NIR) using a UV-1800 Shimadzu Spectrophotometer (Shimadzu, Rigaku-Ko, Japan). Mucin solutions in water–DMSO mixtures were measured using solutions of similar DMSO contents or water as blanks (see individual experiments).

## 3. Results and discussion

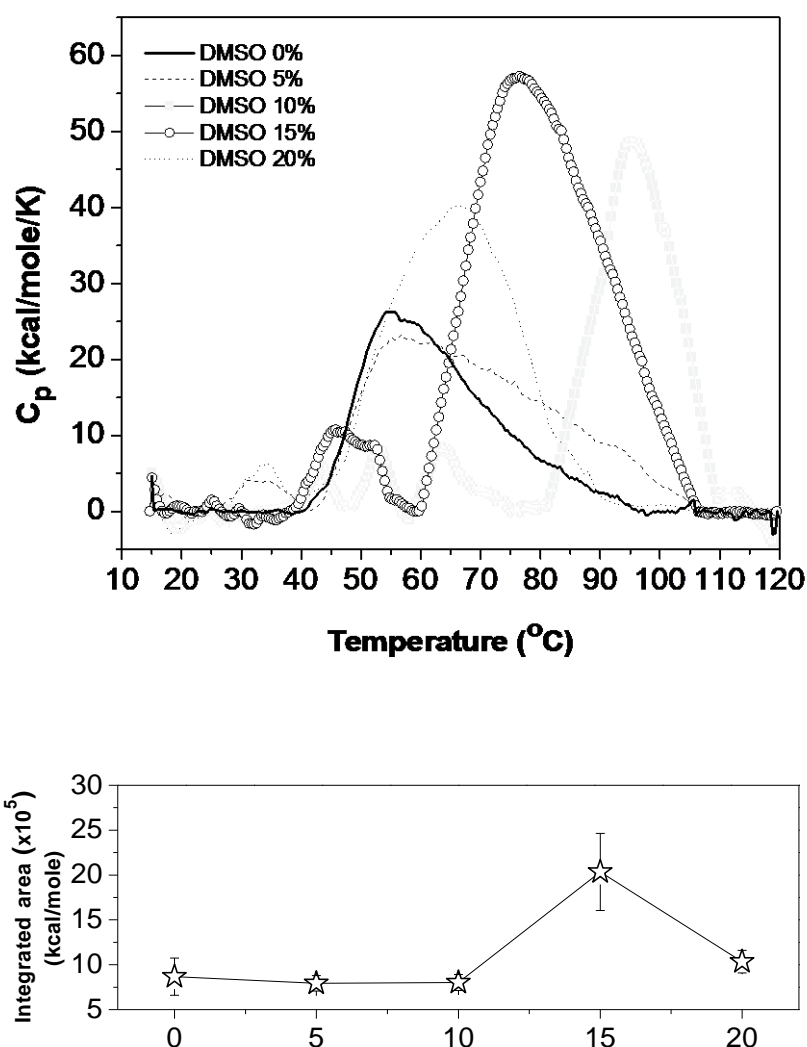
### 3.1 Thermograms in reference to matched solvents

Figure 1 shows the collected data on the thermal events occurring during the heating of 0.1 mg mL<sup>-1</sup> mucin solutions in DMSO (dimethyl sulfoxide)–water solvents with increasing DMSO content (v/v against total solution volume). The same solute-free solvents have also been used as reference materials for these experiments. In the present set of experiments, in the absence of DMSO (water as solvent), an endothermic event manifests as an increase in the molar excess thermal capacity  $C_p$ , starting up at about 40°C, peaking at about 56°C with a maximal  $C_p$  value of 27 kcal (mol K)<sup>-1</sup>, then dropping down until 97°C. The integral of this peak should be the enthalpy corresponding to the observed endotherm, and should be linked to the breaking up of interactions either between the material's components, and/or between them and water, while an increase of the DMSO content will result in the break-up of hydrogen bonds, thus allowing the observation of the latter's effect to the structure of the material under study [7]. Increase of DMSO content to 5% results into two distinct endothermal events: the first one between 26 °C and 38 °C, peaking at 5 kcal (mol K)<sup>-1</sup> and the second one being almost the same event recorded in the absence of DMSO, slightly lower in its maximal  $C_p$ , about 24 kcal (mol K)<sup>-1</sup>, and then tailing down to 115 °C. Wang, Zhang, Zhang, & Ding, (2009) [8] discussed on such double endotherms upon the increase of DMSO content for the case of lentinan, attributing the first ones (observed at about the same temperature range) to transition between two helical structures, while the second one was attributed to the break-up of triple helix to

single strands. Of course, lentinan is a markedly different macromolecule from mucin, and certainly no extrapolations of any sort can be made; however, it is safe to attribute the two endotherms to tertiary or quaternary structural alterations, directly related to the breaking up (and possibly partial assembly) of hydrogen bonding. Further increase of DMSO content to 10% results to the manifestation of four major thermal events: The first three peaks comparable in size to the first, smaller peak of the 5% DMSO scenario (38°C–46°C, 47°C–58°C, 59°C–75°C, all three peaking below 10 kcal (mol K)<sup>-1</sup>); the fourth one is a very large peak between 82°C–110°C, with a maximal  $C_p$  at 46 kcal (mol K)<sup>-1</sup>, that is much higher than the major endotherms observed at lower DMSO content. At 15% DMSO content a double peak appears between 39°C and 56°C, with a maximal  $C_p$  of 6 kcal (mol K)<sup>-1</sup>, which appears to be corresponding to the same events as the two peaks at 38°C–46°C and 47°C–58°C of the 10% DMSO sample. A second, much larger, peak also appears from 60°C to 117°C. The maximal  $C_p$  is at about 56 kcal (mol K)<sup>-1</sup>.

At 20% DMSO, the smaller peak shifts to lower temperatures, and becomes akin to the one noticed for the 5% DMSO sample; while the larger endotherm spans from 40°C–92°C, while the shoulder at the lower temperatures seems like the small peak of the 5% DMSO sample. Overall, the image is characterized by (i) a major peak in the broad range between 60°C and 110°C with a maximal  $C_p$  at some tens kcal (mol K)<sup>-1</sup>, strongly affected by the presence of DMSO (but not its further increase), and (ii) at least three discreet thermal events of a maximal  $C_p$  below 10 kcal (mol K)<sup>-1</sup>, noticed in the broad temperature range between 30°C and 70°C, which arise only in the presence of DMSO. Wang et al. (2009) [8] noticed that such peaks do exist even in the absence of DMSO, but they lie outside the studied temperature range. Figure 1b sums the integrated area results for the range of DMSO contents under study. Concerning the physiological function of mucins, it is easy to notice the sharp onset of an event at just 40°C in the absence of DMSO. Although this is only an *in vitro* experiment, the dramatic changes undergoing by mucin during fever temperatures cannot be left unnoticed: As can be seen in Figure 1, alterations in  $C_p$  are occurring within the range of human temperatures in

health or in inflammation. That is, between 37°C and 40°C, under conditions, mucins could have different thermodynamics between health and disease. Such tantalizing bridges between basic thermodynamics and physiological functionality are largely unstudied and obviously deserve attention; one must note, however, considerations such as the lack of hydration of the samples under study; or that the reproducibility in the shape, half width maximum and onset of the thermal peaks is less consistent than the equivalent reproducibility in area, which make difficult the direct linking of thermodynamic to physiological data.



**Figure 1:** (top) Microthermographs of 0.1 mg mL<sup>-1</sup> mucus solutions DMSO–water mixtures (increasing temperature). DMSO contents (% v/v) appear in the legend; (bottom) Dependence of the



$C_p$  integrated area as a function of DMSO content in the solvent. The blank samples used are DMSO–water mixtures of a composition similar to that of each sample.

It must be noticed that the above endotherms are related to events that occur after DMSO has destroyed most hydrogen bonding connecting mucins to their aqueous environment. So where is all this enthalpy directed to? The observed thermal events are not limited to the break-up of hydrogen bonds, but to the break-up of any interactions which arose from the DMSO-mediated hydrogen bond cleavage. One may assume that mucin is dominated by intermolecular H-bonds, linking the individual sugars with their immediate neighbours within the glycoprotein's tertiary structure. However, DMSO could potentially interfere with the inter-mucin hydrogen bonding network. As DMSO breaks-up the hydrogen bonds connecting mucins with water, it forms a layer around the macromolecules [8-10]. The appearance of a thermal event at low temperatures (as discussed for the first, small peaks above 5% DMSO) should be related to the negation of mucin – DMSO interactions. The strong events at higher temperatures should be obviously linked to the break-up of hydrogen bonds connecting the sugars of the individual macromolecules. As the amount of DMSO increases, the negation of hydrogen bonds between the mucins and water leads mucins to self-assemble into (hydrogen bond-linked) quarternary structures. The increase of  $C_p$  at 10% and 15% DMSO is a confirmation of the creation of such supermolecular structures. Further increase in DMSO results in an excess of DMSO as to break-up such structures, thus lowering the larger endotherm at higher DMSO contents.

### **3.2 Thermograms in reference to water**

The data presented above were obtained using as reference the same DMSO–water mixture that was used as solvent in each case. This provided information on the hydrogen bonding directly affecting mucin. Such data use the presence of DMSO as an instrumental component of the system, as the

DMSO's own thermal effects were negated against the blank. The next step is to review the same phenomena, this time assessing the effect of the excess hydrogen bonding in the reference samples, thus playing out DMSO. To this end, experiments of mucin solutions in DMSO–water solvents were held using blanks without DMSO (plain water). Figure 2 shows the microthermographs for a series of  $0.1 \text{ mg mL}^{-1}$  mucus solutions of varying dimethyl sulfoxide (DMSO) content (v/v against total solution volume), obtained using ultrapure water as reference material. The filled circles correspond to pure water (no DMSO) as solvent. The DMSO-free sample is essentially the same shown in Figure 1, with a thermal event manifesting at about  $40^\circ\text{C}$ , peaking at about  $56^\circ\text{C}$  with a  $C_p$  value of  $27 \text{ kcal (mol K)}^{-1}$ , then dropping down until  $97^\circ\text{C}$ . The integral of this peak should be the enthalpy corresponding to the observed endotherm. In the present case, dissolution of mucus in a 5% v/v DMSO:water solvent (white circles in Figure 2) shows a decrease in both the onset temperature (about  $31^\circ\text{C}$ ) and the maximum attained  $C_p$  value ( $17 \text{ kcal (mol K)}^{-1}$ ), as well as a lower integrated area (enthalpy). The thermal event terminates at about  $97^\circ\text{C}$ , that is the same temperature as in the absence of DMSO. Further increase of the DMSO content in the solvent (10% DMSO, filled triangles in Figure 2) results in a reduction of the maximum attainable  $C_p$  (about  $7 \text{ kcal (mol K)}^{-1}$ ) and a reduction in the overall area (enthalpy), while the onset of this thermal event is at about  $45^\circ\text{C}$  and carries on well after the lower DMSO samples, at about  $110^\circ\text{C}$ .

In terms of absolute enthalpy, at 0% and 5% DMSO, the recorded values are in the order of size as those obtained for okra polysaccharide, a strong thickener [6]; while at higher values, this further increase in DMSO at 15% or at 20% of the solvent results to a dramatic decrease of excess heat capacity and enthalpy, e.g.  $C_p$  drops from  $7 \text{ kcal (mol K)}^{-1}$  to  $0.5 \text{ kcal (mol K)}^{-1}$  for 15% DMSO and  $0.2 \text{ kcal (mol K)}^{-1}$  for 20% DMSO, the widths of the respective peaks remain unchanged (see Figure 2, inset).

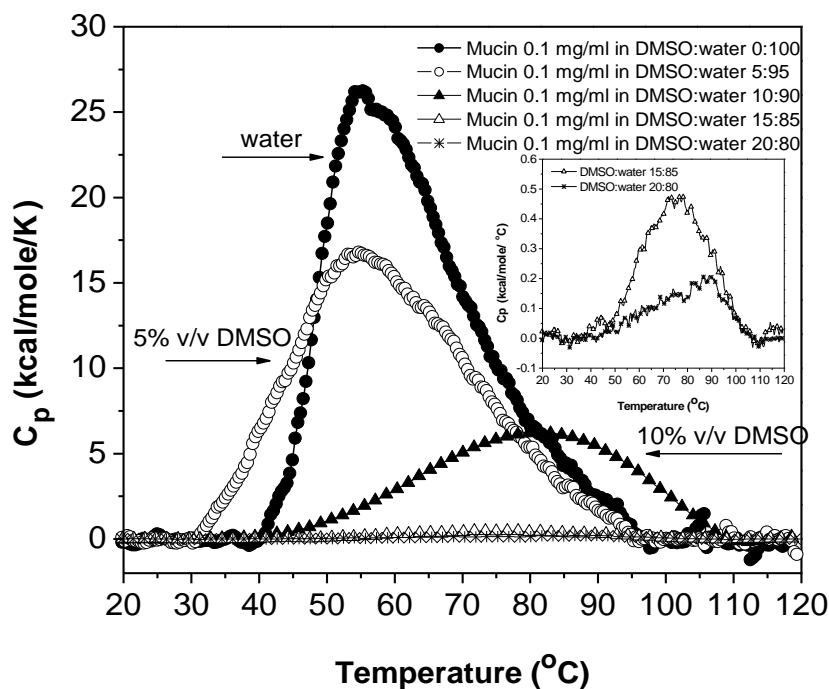
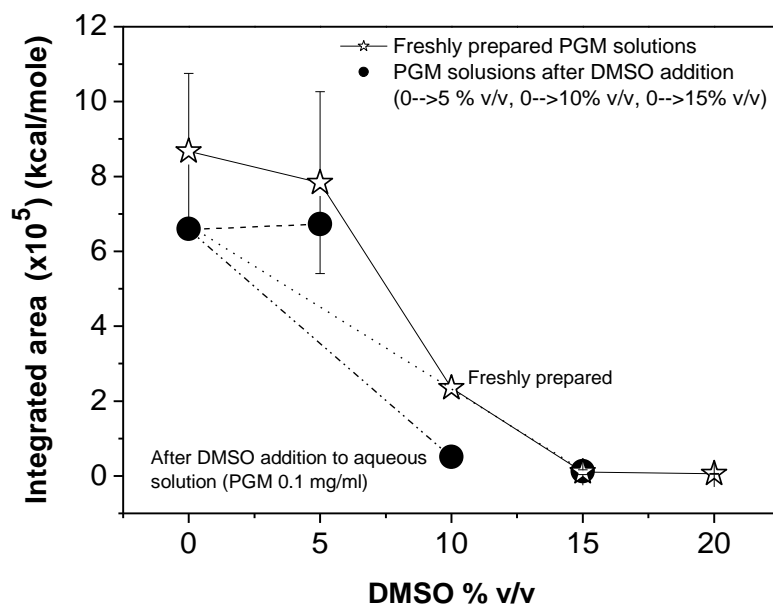


**Figure 2:** Microthermographs of  $0.1 \text{ mg mL}^{-1}$  mucus solutions DMSO–water mixtures (increasing temperature). The blank sample used is water. Data for some water / DMSO contents are plotted as an inset graph as to avoid congestion in the main figure.

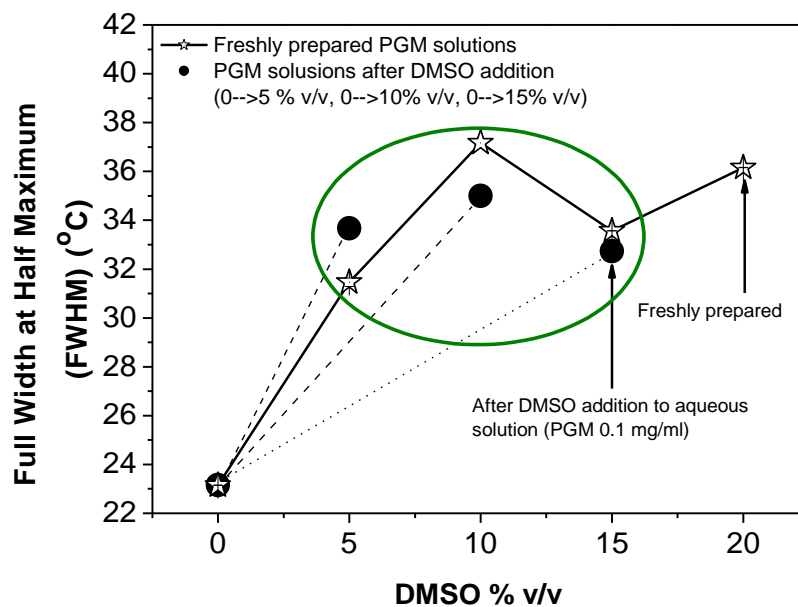
Assuming that the observed alterations in  $C_p$  are directly attributable to thermal events due to the break-up of interactions, and that the presence of DMSO breaks hydrogen bonds and will not interfere in other ways to the thermal properties of the material under study, one may make the following statements: (i) The differences between the 0% DMSO and the other samples are due to the breaking-up of hydrogen bonds, and these bonds can be quantified in the form of differences between in the integrals of the respective  $C_p$ – $T$  curves; (ii) the shift at the onset of the endotherms, e.g. between 0 and 5% DMSO is due to the re-allocation of hydrogen bonds to places which are more easily broken up (e.g. in non-sterically encumbered places); (iii) conversely, shifts to higher temperatures (as in the samples of 10% DMSO or above) are due to the allocation of hydrogen bonds to more protected positions. According to the above, hydrogen bonds appear to be breaking up in a

consistent manner with the increase in DMSO concentration. Figure 3 (top) shows a plot of the integrated area (essentially the enthalpy of the broken bonds), where can be seen that there exists a monotonic but not linear decrease in enthalpy, hence extent of hydrogen bonding. Practically all bonds that break are already destroyed at about 15% v/v DMSO. In a similar trend, the maximum attainable  $C_p$  also drops from 27 kcal (mol K)<sup>-1</sup> in the absence of DMSO to 0.5 kcal (mol K)<sup>-1</sup> at 15% v/v DMSO (Figure 2). The reduction in excess heat capacity is due to the break-up of the hydrogen bonds.

According to the recent literature for other biomacromolecules [6,8] increase in DMSO results in increases of  $C_p$  and enthalpy up to a (low) DMSO content; then  $C_p$  and enthalpy both decrease down to their elimination. This is clearly not followed in the present case, where the measured quantities decrease in a smooth, monotonic fashion; moreover, the width of the  $C_p$  curve, expressed here as the half width at maximum, is fairly constant throughout the DMSO range under study (Figure 3 bottom). The rise-and-fall patterns of enthalpy with DMSO content in okra pectin and lentinan were attributed to the initial rearrangement of the hydrogen bond network from one between the polymers in self-associated structures to one between individual polysaccharides and water [6], and to the formation of a protective layer of DMSO molecules around the polymeric entities [7], along with the creation of new hypermolecular structures held together by new hydrogen bonds. In the present case, however, the smooth transition of  $C_p$  from high to negligible values with DMSO content, and the stability of the width imply an equally smooth sequence of events, which will not involve other than the steady break-up of hydrogen bonds with DMSO. This suggests that, once broken, hydrogen bonds will not be re-formed between new units in the polymeric chains in the present experiments; that is, mucin chains should not be in flexible conformations or in dense three-dimensional structures.



(a)



(b)

**Figure 3:** Dependence of the  $C_p$  integrated area (top) and the full width at half maximum (FWHM) (bottom) as a function of DMSO content in the solvent. Stars denote solutions where mucus was dissolved in DMSO–water solutions of a given DMSO content. Circles denote solutions prepared by

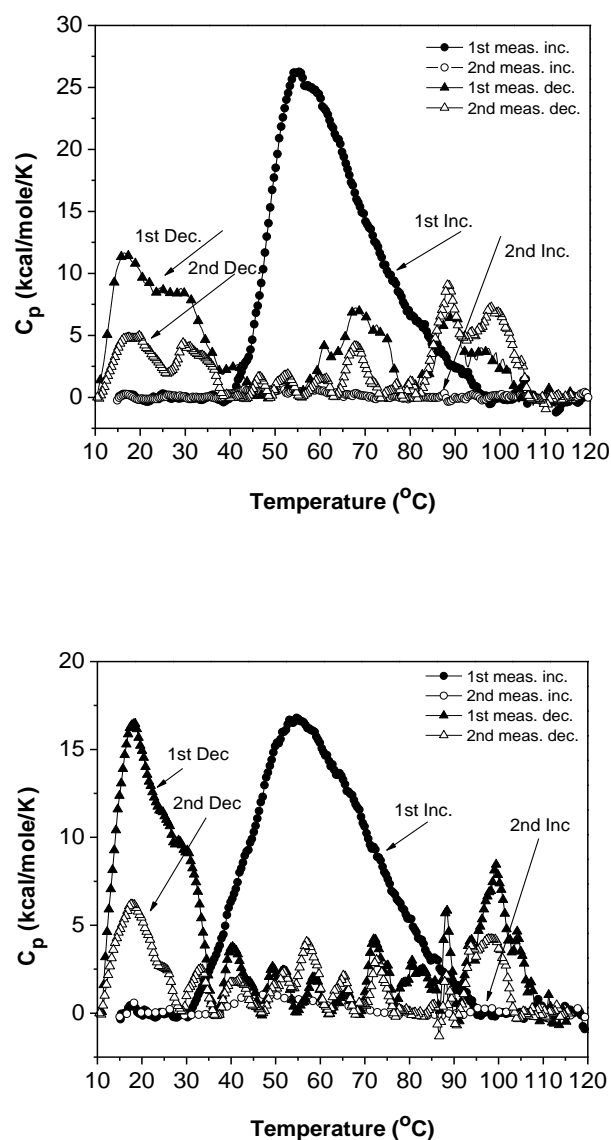
adding DMSO into existing aqueous mucin solutions. The blank sample used is water.

Figure 3 (top and bottom) shows the results of another set of experiments (“dilutions”), in which DMSO was added into water until its content was brought to a desired level, the mucus concentrations were re-calculated, and the experiments were resumed. The top plot shows that the addition of DMSO to a level of 5% v/v did not result into a substantial change in overall  $C_p$  (the integral of the endotherm remains roughly the same); assuming that changes in  $C_p$  reflect changes in the overall enthalpy stored in H-bonding, one can conclude that DMSO did not alter the self-assembly of bulk water (the reader should be reminded that the reference is water, so  $\Delta C_p$  reflects changes in the H-bonding of bulk water, too). That suggests that DMSO may, upon its addition into an existing mucus solution, remain phase-separated as to exert minimal interference with the existing bonding.

The actual localization of this phase separation is hinted in Figure 3 (bottom), where a small increase in the full width at half maximum (FWHM) is observed with the same DMSO addition; this parameter is a good indicator for the polydispersity of the interactions, as a peak widening (here FWHM) suggests different bonds which break up at different temperatures. Still, as can be seen in the y-scale, this parameter does not alter much as compared to the overall area (the most important parameter). Development of limited bond polydispersity upon DMSO addition suggests that the H-bonding network is somehow re-arranged; as the bulk water does not appear to play part in this (see above), the most plausible explanation combining the consistency in  $C_p$  and increase in FWHM is that the DMSO–water phase separation occurs at the mucin surface, where DMSO actively re-arranges the H-bonding network of the glycoprotein. This is in complete agreement with the suggested DMSO interfacial layer on the mucin macromolecules.

### 3.3 Temperature cycling

A question that arises next, as a direct consequence of the above is about the equilibrium character of the mucin H-bond-mediated structures: Is the mucin native state thermodynamically favorable, or it is closer to what can be described as pseudo-equilibrium?



**Figure 4:** Microthermographs of 0.1 g dL<sup>-1</sup> mucin solutions in water (top) and 5 % v/v DMSO–water (bottom) under heating–cooling cycles (two cycles with increasing “Inc” and decreasing “Dec” temperature). The blank sample used is water.

In order to investigate this, mucin solutions underwent two successive 10<sup>o</sup>C–120<sup>o</sup>C–10<sup>o</sup>C

temperature cycling routines. These were performed for pure water and 5% DMSO solvents (Figure 4, top and bottom plots, respectively). For reasons of direct comparability, water has been used as blank in both cases. In the first increasing temperature run, mucin solvated in pure water shows the strong thermal event described previously. The following drop in temperature leads to three thermal events, manifesting as  $C_p$  peaks centred around 95°C, 70°C and 20°C (Figure 4 top). The overall enthalpy associated to these events (proportional to the peak area) is lower than the one observed for the single endotherm of the rising temperature run. A second run performed after a reasonable equilibration time (several hours) shows no significant peaks; while the second temperature drop, interestingly, is essentially similar to the one of the first temperature receding run (although the peaks are of somehow different  $C_p$  values).

A similar image is observed in the presence of 5% DMSO in the solvent (Figure 4 bottom): The major thermal event observed during the first increasing temperature run is never repeated; while the less prominent thermal events observed during the decreasing temperature stages are fairly reproducible in the consecutive decreasing temperature run.

The above suggest that, at least as far as endothermic events are concerned, the start-up structures, when thermally forced to absorb thermal energy and then relax, end up in relatively stable thermal states; these latter are, due to their reproducible thermal behavior (and smaller associated energies), closer to what one would call “equilibrium structures”. Under a similar rationale, the initial states could be described as “pseudo-equilibria”; however, the above are merely indications: a definite answer in the native mucin equilibrium or pseudo-equilibrium state cannot be given based on the present data alone.

### **3.4 UV-vis-NR spectroscopy measurements**

The samples were examined in the form of mucin solutions of varying DMSO–water content, using as reference samples (blanks) either (i) water, or (ii) DMSO–water mixtures of the same composition



as in the mucin samples under study. Within near-infrared, absorbance reductions are due to the loss of conjugation or due to chromophore rearrangements. As no covalent bonds are expected to break-up from the mild conditions used in this study, any loss of conjugation would be due to the re-arrangement or break up of other bonds (e.g. H-bonds) in the vicinity of conjugated structures. In that sense, one would be able to detect the spatial rearrangements between conjugated regions of the macromolecules, hence changes in hydration or other solvation phenomena. Figure 5 (top) shows results for case (i) (water as reference). It can be seen that a major peak dominates the near UV region (max at about 260 nm). In UV spectroscopy proper, this is easily attributable to a sequence of about two to four conjugated double bonds, typically an aromatic amino-acid, in this case, most possibly, out of the protein backbone of mucin. However, upon increase in DMSO content, this peak diminishes in size. A question arises: Is this because the aromatics–water H-bonds are taken out by DMSO, or because the entire solvent changes its absorption characteristics due to DMSO interference with the bulk water network?

To address the above, increase of DMSO content into mucin solutions results into a dramatic loss of absorbance in this region, at even lower absorbance values than solutions of the same initial DMSO–water content (see Figure 5, top, plots at the bottom). This clearly suggests that the interference of DMSO is essentially local, directly interfering with the aromatic (aminoacids) vibration, that is further reinforcing the argument of a DMSO layer attached onto the macromolecules' surface.

One could take advantage of such a DMSO layer as to study the local thermodynamics of the chain mobility, this time negating the DMSO effect by matching the solvent with the reference sample (case (ii), Figure 5 bottom): In this scenario, with the DMSO effects negated from a spectroscopy point of view, a blue shift (rightward shift of the absorption maximum) becomes clear as the DMSO content increases, that is as H-bonding decreases.

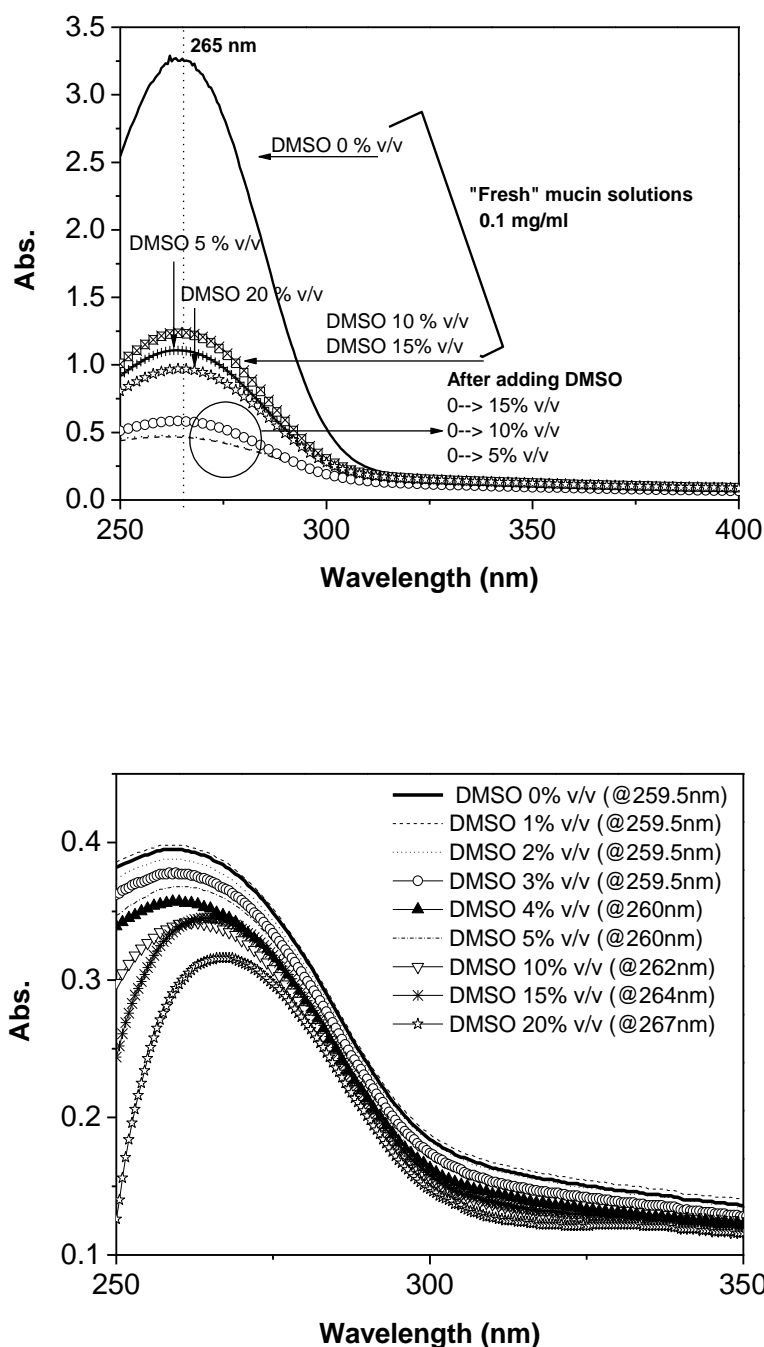


**Figure 5:** Near-UV spectra of 0.1 mg mL<sup>-1</sup> mucus solutions DMSO–water mixtures. The blank samples used are water (top) and DMSO–water mixtures of a composition similar to that of each sample (bottom). In all cases (top and bottom), solutions were prepared by dissolving mucus in DMSO–water solutions of a given content (without adding further DMSO). Only the three lower

plots in the upper graph denote solutions prepared by means of adding DMSO into existing mucus solutions up to the desired DMSO content (highlighted in circle).

This suggests that the chromophores (here conjugated aminoacids) are restricted in their mobility by the presence of hydrogen bonds. As these are negated (here by DMSO), the amino acid mobility increases (hence the shift to higher wavelengths). That can be interpreted as follows: In an aqueous environment, the aromatic amino acids of mucin (hence the protein backbone chain) are restricted in their movement by hydrogen bonds. Since the most readily available H-bonds are the bonds between adjacent sugar moieties, these should play a role in stabilizing the entire polymer chain. That suggests that the inherent stability of mucin is not only due to steric volume exclusions, but also by means of extensive hydrogen bonding on behalf of the sugar moieties.

#### **4. Conclusions**

- Formation and break-up of hydrogen bonding has been monitored in mucus solutions.
- The sugar moieties directly involved in hydrogen bonding play a substantial role in mucin self-assembly.
- Mucus is dominated by intermolecular H-bonds, apparently linking the individual mucins' sugars with their immediate neighbours within the glycoprotein's tertiary structure.
- DMSO could potentially interfere with the inter-mucin hydrogen bonding network, breaking up the hydrogen bonds connecting mucins with water, and forming a layer around the macromolecules.
- As the amount of DMSO increases, the negation of hydrogen bonds between the mucins and water leads mucins to self-assemble into (hydrogen bond-linked) quaternary structures; while further increase in DMSO results in an excess of DMSO as to break-up such structures.

- Once broken, hydrogen bonds will not be re-formed between new units in the polymeric chains in the present experiments; that is, mucin chains should not be in flexible conformations or in dense three-dimensional structures.
- A blue shift of the conjugated aminoacids in the presence of DMSO suggests that the inherent stability of mucin is not only due to steric volume exclusions, but also by means of extensive hydrogen bonding on behalf of the sugar moieties.

**Acknowledgment:**

Support of the Zhejiang Province, China, through the Thousand Talents Program is acknowledged.

**References**

- [1] A.N. Round, N.M. Rigby, A. Garcia de la Torre, A. Macierzanka, E.N. Clare Mills, A. R. Mackie, Lamellar Structures of MUC2-Rich Mucin: A Potential Role in Governing the Barrier and Lubricating Functions of Intestinal Mucus, *Biomacromolecules* 13 (10) (2012) 3253–3261.
- [2] K. Jumel, I. Fiebrig, S.E. Harding, Rapid size distribution and purity analysis of gastric mucus glycoproteins by size exclusion chromatography/multi angle laser light scattering, *Int. J. Biol. Macromol.* 18 (1996) 133–139.
- [3] M.E.V. Johansson, H. Sjövall, G.C. Hansson, The gastrointestinal mucus system in health and disease, *Nat. Rev. Gastroenterol. Hepatol.* 10(6) (2013) 352–361.
- [4] O. Svensson, T. Arnebrant, Mucin layers and multilayers—Physicochemical properties and applications, *Curr. Opin. Colloid Interface Sci.* 15 (2010) 395–405.
- [5] A.P. Corfield, Mucins: A biologically relevant glycan barrier in mucosal protection, *Biochimica et Biophysica Acta* 1850 (2015) 236–252.
- [6] S. Lousinian, M. Dimopoulou, C. Panayiotou, C. Ritzoulis, Self-assembly of a food hydrocolloid: The case of okra mucilage, *Food Hydrocolloids* 66 (2017) 190–198.

- [7] X. Xu, X. Wang, F. Cai, L. Zhang, Renaturation of triple helical polysaccharide lentinan in water-diluted dimethylsulfoxide solution, *Carbohydr. Res.* 345 (2010) 419–424.
- [8] X. Wang, Y. Zhang, L. Zhang., Y. Ding, Multiple Conformation Transitions of Triple Helical Lentinan in DMSO/Water by Microcalorimetry, *J. Phys. Chem. B* 113 (2009) 9915–9923.
- [9] M. Avgidou, M. Dimopoulou, A.R. Mackie, N.M. Rigby, C. Ritzoulis, C. Panayiotou, Physicochemical aspects of mucosa surface, *RSC Advances* 6 (2016) 102634–102636.
- [10] X. Wang, X. Zhang, X. Xu, L. Zhang, The LiCl effect on the conformation of lentinan in DMSO, *Biopolymers* 97 (2012) 840-845.

**Captions to illustrations**

**Figure 1:** (top) Microthermographs of  $0.1 \text{ mg mL}^{-1}$  mucus solutions DMSO–water mixtures (increasing temperature). DMSO contents (% v/v) appear in the legend; (bottom) Dependence of the  $C_p$  integrated area as a function of DMSO content in the solvent. The blank samples used are DMSO–water mixtures of a composition similar to that of each sample.

**Figure 2:** Microthermographs of  $0.1 \text{ mg mL}^{-1}$  mucus solutions DMSO–water mixtures (increasing temperature). The blank sample used is water. Data for some water / DMSO contents are plotted as an inset graph as to avoid congestion in the main figure.

**Figure 3:** Dependence of the  $C_p$  integrated area (top) and the full width at half maximum (FWHM) (bottom) as a function of DMSO content in the solvent. Stars denote solutions where mucus was dissolved in DMSO–water solutions of a given DMSO content. Circles denote solutions prepared by adding DMSO into existing aqueous mucin solutions. The blank sample used is water.

**Figure 4:** Microthermographs of  $0.1 \text{ g dL}^{-1}$  mucus solutions in water (top) and 5 % v/v DMSO–water (bottom) under heating–cooling cycles (two cycles with increasing “Inc” and decreasing “Dec” temperature). The blank sample used is water.

**Figure 5:** Near-UV spectra of  $0.1 \text{ mg mL}^{-1}$  mucus solutions DMSO–water mixtures. The blank samples used are water (top) and DMSO–water mixtures of a composition similar to that of each sample (bottom). In all cases (top and bottom), solutions were prepared by dissolving mucus in DMSO–water solutions of a given content (without adding further DMSO). Only the three lower

plots in the upper graph denote solutions prepared by means of adding DMSO into existing mucus solutions up to the desired DMSO content (highlighted in circle).

**Highlights**

- Microcalorimetry is used to study mucin self-assembly.
- Formation and break-up of hydrogen bonding has been monitored in mucus solutions.
- Sugar moieties play a substantial role in mucin self-assembly.
- Metastable pseudo-equilibria appear to dominate mucin self-assembly.